MOTION NEAR THE TRANSITION TO COMPLEX INSTABILITY: SOME EXAMPLES

MERCÉ OLLÉ[(1)], JUAN R. PACHA[(1)]

(1) Departament de Matemàtica Aplicada I, Universitat Politècnica de Catalunya, Diagonal 647, 08028 Barcelona (España)

Abstract

Complex instability is a generic kind of instability in Hamiltonian systems with three or more degrees of freedom. In this work, some examples of such instability are shown, together with a numerical analysis of the dynamics close to the transition from stability to complex instability for a family of periodic orbits.

1 Parametric stability and eigenvalues collision on the unit circle

Let $T : \mathbb{R}^4 \mapsto \mathbb{R}^4$, be a symplectic map, with $T(0) = 0$. Then its jacobian matrix at the origin, $A = DT(0)$, will be a symplectic matrix. It is well known (see [1]), that if $\lambda, \mu \in \mathrm{spec}\,(A)$, then also $1/\lambda, 1/\mu \in \mathrm{spec}\,(A)$, so the condition for the origin to be an stable fixed point, is that each eigenvalue lies on the unit circle. Eventually, the map T could depend on one parameter, σ, in such a way that, for $\sigma < 0$ the two reciprocal pairs of eigenvalues are on the circle, for $\sigma = 0$ a pairwise collision of eigenvalues takes place, and at last, for positive values of the parameter, the eigenvalues leave the unit circle by reciprocal pairs. See figure 1 for an illustration of the global process. At the transition from stability to complex instability the eigenvalues are equal by pairs, so by their reciprocity also:

$$\lambda = \mu = e^{i2\pi k}, \qquad \frac{1}{\lambda} = \frac{1}{\mu} = e^{-i2\pi k}.$$

In order to study the linear stability of 4D-symplectic mappings, some quantities related with the eigenvalues of the matrix A are introduced (see [2], [5]):

- *Stability Parameters.* Defined by: $b_1 = -(\lambda + 1/\lambda)$, and $b_2 = -(\mu + 1/\mu)$.
- *Stability Coefficients*: $\alpha = b_1 + b_2$, $\beta = 2 + b_1 b_2$.
- *Discriminant*: $\Delta = (b_1 - b_2)^2$.

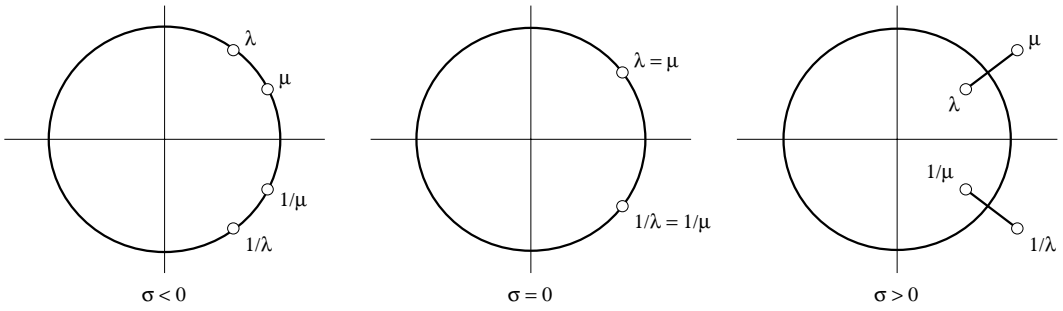

Figure 1: Transition stable complex-unstable

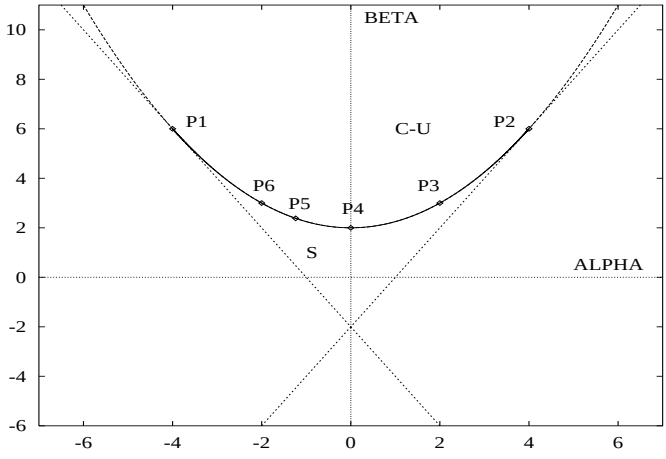

Figure 2: Transition Stable-$\mathbb{C}$U on the Broucke Diagram.

The fixed point is stable if $|b_1| \leq 2$, $|b_2| \leq 2$, or complex-unstable if $\Delta < 0$ and $b_1, b_2 \in \mathbb{C}$, while the transition takes place when $\Delta = 0$, or in terms of the stability coefficients, when:

$$\alpha = -4\cos(2\pi k), \qquad \beta = 2 + 4\cos^2(2\pi k) \tag{1}$$

and this happens along the parabolic arc from P_1 to P_2 on the Broucke diagram (figure 2). See [2].

Linked to this change of stability, there is a characteristic type of bifurcation; the so called *Hopft-like* bifurcation, for which the bifurcating objects are different depending upon the rotation number k at the transition (1). More precisely: if $k = m/n \in \mathbb{Q}$ or $k \in \mathbb{R} \setminus \mathbb{Q}$, n periodic orbits or invariant curves surrounding the fixed point, respectively, may bifurcate. Furthermore, if the bifurcating objects unfold on the unstable side, then they are stable (*direct* bifurcation). Otherwise, when the bifurcation unfolds towards the stable side, the objects are unstable (*inverse* bifurcation).

The effect of the direct bifurcation is to confine the phase space so the consequents, $T^n(x_0)$ of a point x_0 close to the fixed point 0, remain in a domain surrounding the fixed point for large values of n. The inverse bifurcation occurs on the stable side, so the consequents of the unstable side are not confined. The effect of the inverse bifurcation is

more subtle: it compresses the stable curves around the fixed point, so their number is reduced.

In fact, the phenomenon described in this last paragraph gives us a key to find out if the system undergoes direct or inverse bifurcation: we shall test if the consequents of points on the unstable side are confined. If so, this indicates that direct bifurcation is taking place. Otherwise, we may expect, at most, inverse bifurcation.

In the next section we shall study a couple of mappings, which exhibit all the features related with the transition from stability to complex instability. In the last two sections, these ideas are applied to Hamiltonian systems.

2 Froeschlé's generalized mappings

In order to describe the generic behaviour linked to the transition, let us consider the 4D T_s and T_t mappings (see [5]) around $x = 0$, fixed point. They are defined by:

$$T_s \begin{bmatrix} x_1 \\ x_2 \\ x_3 \\ x_4 \end{bmatrix} = \begin{bmatrix} D\left[x_1 + K_1 \sin\left(x_1 + x_2\right) + L_1 \sin\left(x_1 + x_2 + x_3 + x_4\right)\right] \\ x_1 + x_2 \\ D\left[x_3 + K_2 \sin\left(x_3 + x_4\right) + L_2 \sin\left(x_1 + x_2 + x_3 + x_4\right)\right] \\ x_3 + x_4 \end{bmatrix} \bmod(2\pi) \qquad (2)$$

and:

$$T_t \begin{bmatrix} x_1 \\ x_2 \\ x_3 \\ x_4 \end{bmatrix} = \begin{bmatrix} D\left[x_1 + K_1 \sin\left(x_1 + x_2\right) + L_1 \tan\left(x_1 + x_2 + x_3 + x_4\right)\right] \\ x_1 + x_2 \\ D\left[x_3 + K_2 \sin\left(x_3 + x_4\right) + L_2 \tan\left(x_1 + x_2 + x_3 + x_4\right)\right] \\ x_3 + x_4 \end{bmatrix} \bmod(2\pi). \qquad (3)$$

Let $A = DT_\nu(0)$ $(\nu = s, t)$, then:

$$A = \begin{pmatrix} 1 + L_1 + K_1 & L_1 + K_1 & L_1 & L_1 \\ 1 & 1 & 0 & 0 \\ L_2 & L_2 & 1 + L_2 + K_2 & L_2 + K_2 \\ 0 & 0 & 1 & 1 \end{pmatrix}$$

(for $D = 1$). Then it is easy to see that:

$$\Delta = \alpha^2 - 4\beta + 8 = (K_1 - K_2 + L_1 - L_2)^2 + 4L_1L_2.$$

The Froeschlé's mapping corresponds to (2) with $L_1 = L_2$, but then, the discriminant $\Delta > 0$, so no complex instability is possible at all. Instead, we restrict the parameter space by taking $L_1 = -L_2 = -L$, $K_1 = K$, and $K_2 = 0$. Now $\Delta = K(K + 4L)$. If $-8 < K < 0$, we have that for $L < -K/4$, the origin 0 is an stable fixed point and for $L > -K/4$, the origin is complex-unstable. The transition takes place at $L = L_{Crit} = -K/4$, $(\Delta = 0)$.

Now, for each fixed K in the interval $-8 < K < 0$, we may vary L continuously from $L < L_{Crit}$ to some value $L > L_{Crit}$ and explore what happens in the neighbourhood of L_{Crit}. D is a dissipative parameter introduced for computational purposes (see the explanation below).

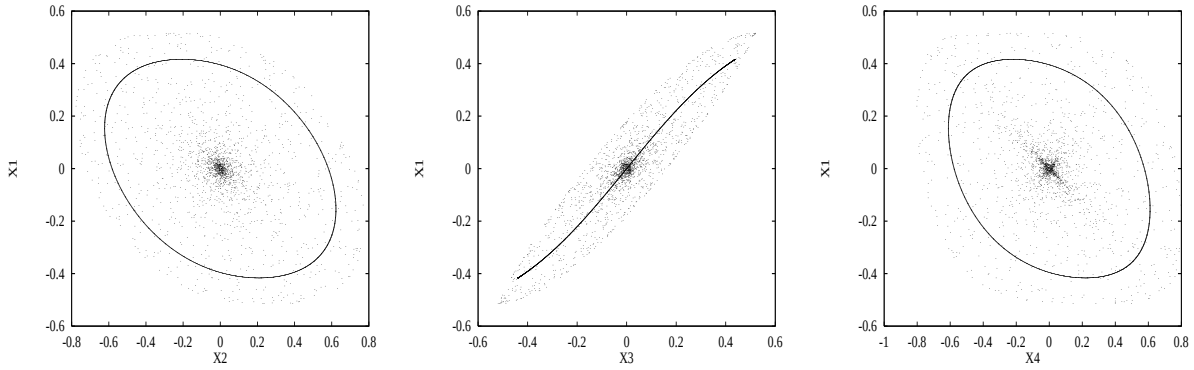

Figure 3: Confinement of the stochastic points around the complex-unstable fixed point, in the mapping T_s at $K = -1$, $L = 0.28$.

Numerical simulations show that for the T_s mapping, the bifurcation is of direct type while, for the T_t mapping the bifurcation is inverse. In [5], an extensive study of the bifurcation to periodic orbits and invariant curves has been made both for T_s and for T_t. The study of the evolution and further bifurcations of such invariant curves was carried out in [3]. In figure 3 we reproduce an invariant curve which bifurcate on the unstable side for $K = -1$ and $L = 0.28 > L_{Crit}$, as well as the confinement of the stochastic points around the complex unstable fixed point.

The invariant curves were found by the "dissipative method": these become attracting limit cycles as the parameter D is $D < 1$, so one starts with a value of D less than one, and calculates the consequents of a point. The consequents converge rapidly onto an invariant curve (in fact, onto a limit cycle) while $D < 1$. Hence, increasing smoothly the dissipative parameter until $D = 1$, the desired invariant curve is finally reached.

3 The restricted three body problem

Now we consider the vertical family of periodic orbits of the restricted three-body problem around the triangular Lagrange point L_4. From the study of the stability of this family (see figure 4), it is clear that, for an interval of the mass parameter, $\mu_{Routh} < \mu \lesssim 0.12$, the vertical family reaches complex instability.

For the analysis of the stability, we reduce the three degrees of freedom Hamiltonian system to a 4D symplectic mapping, by the use of the Poincaré map T, with $\{z = 0\}$ as a surface of section, and by fixing the energy level of each orbit. In this way, the study of the stability of a two parameter (μ, p_z) family of periodic orbits, is reduced to the corresponding study for a family (depending upon the same parameters) of fixed points of the map T.

In order to find out what type of bifurcation takes place from the transition, we consider an orbit close to a complex-unstable periodic orbit of the family. The consequents by T are confined for a large number of iterates. Therefore, the bifurcation is direct and the existence of the invariant curves is expected. We computed them by means of the dissipative method and we show one of them in figure 5.

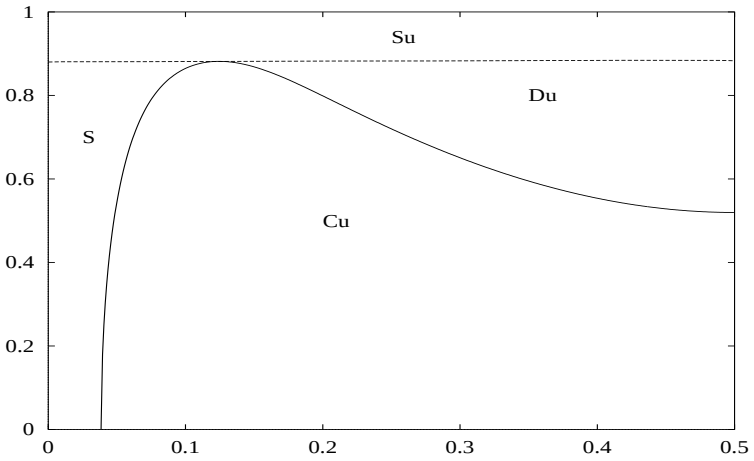

Figure 4: Change of the linear stability of the vertical family of L_4. the values of $\dot{z} = p_z$, when $z = 0$ are plotted against the mass parameter μ. The Su and Du in the figure stand for *simple-unstable* and *double-unstable*.

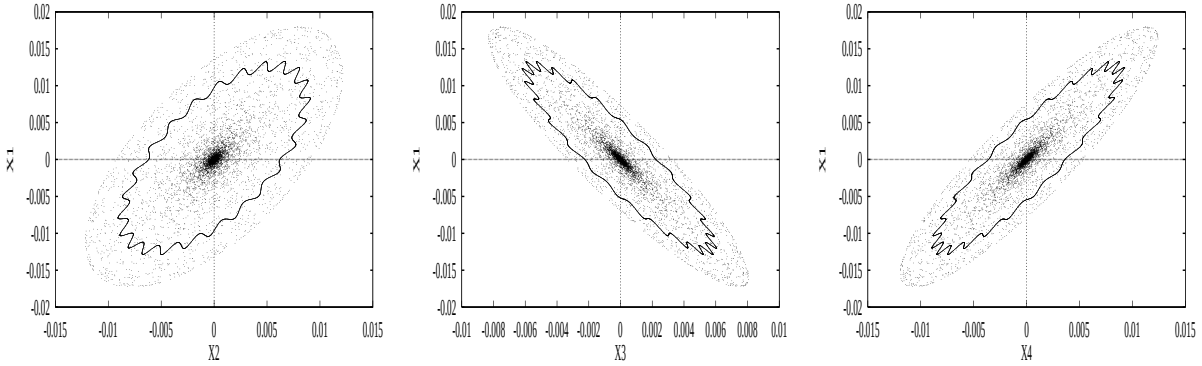

Figure 5: Confinement and invariant curves of the direct bifurcation in the RTBP.

4 Barred galactic model potential

We consider the Miyamoto-Ferrers galactic model for a barred galaxy, given by the Hamiltonian:

$$H = \frac{1}{2}\left(p_x^2 + p_y^2 + p_z^2\right) + \Phi(x, y, z) - \Omega\left(xp_y - yp_x\right), \quad \Phi = \Phi_D + \Phi_B$$

where Φ_D and Φ_B stands for the contribution of the disk and the bar to the global galactic potential. As in the RTBP, this system has five equilibrium points: three collinear and two triangular (noted also by L_1, L_2, L_3, and L_4, L_5). The stability of the vertical family of periodic orbits around L_4 has been studied in [4]. In fact, this study is parallel to the one done for the RTBP. Nevertheless, for the galactic potential, there appear a transition stable complex-unstable with a bifurcation of inverse type.

To see the effect of this bifurcation on the invariant tori surrounding the stable central family, an *anti-dissipative* parameter D slightly larger than 1 is introduced in such a way

that the system becomes volume dilating, but conserving the Hamiltonian. If we take initial conditions on the stable side, we must note that, in the original Hamiltonian case, the orbit lies on a torus, but due to the presence of the anti-dissipative perturbation D, the consequents of an initial point on the surface of section $z = 0$ (if we think in terms of the Poincaré map), explore larger and larger tori until they reach the last one, and a sudden escape takes place. So, this provides us with an upper bound of the extent of the invariant tori: these bounds are easily seen looking at the shell formed by the accumulated points just before the escape (see figure 6).

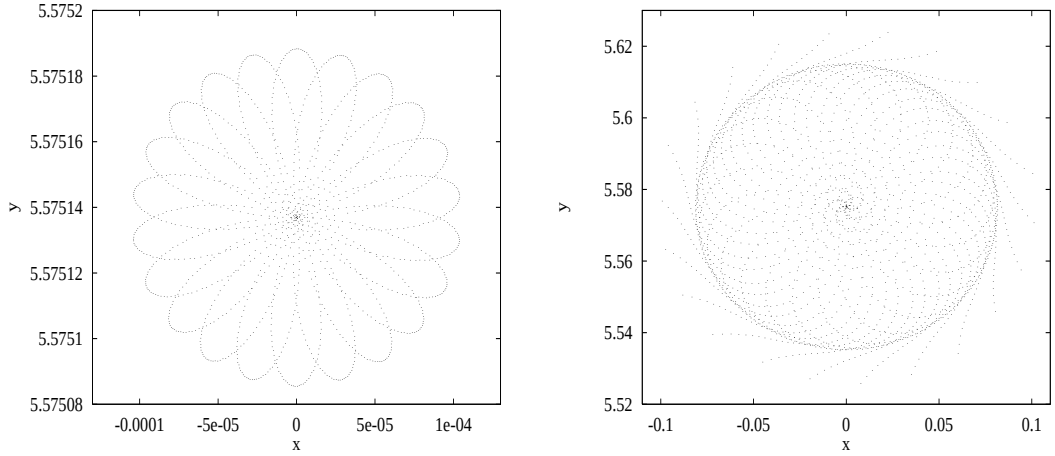

Figure 6: Left: (x, y) projection of the consequents of an orbit in the Poincaré section $z = 0, p_z > 0$. Right: the envelope formed by the consequents of the anti-dissipative perturbed system just before the escape. The same initial conditions are taken in both cases.

References

[1] V. I. Arnold, *Méthodes Mathématiques de la Mécanique Classique*, Éditions Mir, Moscou, 1974.

[2] R. Broucke "Stability of periodic orbits in the elliptic, restricted three body problem", *AIAA Journal*, **32**, (1969), 1003-1009.

[3] M. Ollé and D. Pfenniger, "Bifurcation at complex instability", *Proceedings NATO ASI Adv. Sci. Inst. Ser. C Math. Phys. Sci.*, en S'Agaró, España, Junio 1995, Kluwer Acad. Publ. Dordrecht, Holland.

[4] M. Ollé and D. Pfenniger, "The vertical orbital structure around the Lagrangian points in barred galaxies", to appear in *Astron. Astrophys.*

[5] D. Pfenniger, "Numerical study of complex instability I. Mappings", *Astron. Astrophys.*, **150**, (1985), 97-111.